Characterization of the Liquid-Ordered State by Proton MAS NMR

Ivan V. Polozov and Klaus Gawrisch
Laboratory of Membrane Biochemistry and Biophysics, National Institute on Alcohol Abuse and Alcoholism, National Institutes of Health, Bethesda, Maryland 20892

ABSTRACT We investigated if magic angle spinning (MAS) ^{1}H NMR can be used as a tool for detection of liquid-ordered domains (rafts) in membranes. In experiments with the lipids SOPC, DOPC, DPPC, and cholesterol we demonstrated that ^{1}H MAS NMR spectra of liquid-ordered domains (l_o) are distinctly different from liquid-disordered (l_d) and solid-ordered (s_o) membrane regions. At a MAS frequency of 10 kHz the methylene proton resonance of hydrocarbon chains in the l_d phase has a linewidth of ~50 Hz. The corresponding linewidth is ~1 kHz for the l_o phase and several kHz for the s_o phase. According to results of ^{1}H NMR dipolar echo spectroscopy, the broadening of MAS resonances in the l_o phase results from an increase in effective strength of intramolecular proton dipolar interactions between adjacent methylene groups, most likely because of a lower probability of *gauche*/*trans* isomerization in l_o. In spectra recorded as a function of temperature, the onset of l_o domain (raft) formation is seen as a sudden onset of line broadening. Formation of small domains yielded homogenously broadened resonance lines, whereas large l_o domains (diameter >0.3 μm) in an l_d environment resulted in superposition of the narrow resonances of the l_d phase and the much broader resonances of l_o. ^{1}H MAS NMR may be applied to detection of rafts in cell membranes.

INTRODUCTION

Cholesterol is a major component of eukaryotic biomembranes and a known modulator of lipid phase behavior. The concept of lipid rafts (1), lateral domains in membranes of elevated cholesterol, and glycosphingolipid content that play an important role in cell signaling has renewed interest in the study of membrane lateral organization. Although biochemical evidence for existence of rafts is strong, detection of the structural equivalent of a raft in biomembranes has proven to be extremely difficult.

It was proposed that rafts are domains of a liquid-ordered phase, surrounded by a liquid-disordered lipid matrix. The liquid-ordered phase concept has been put forward by Ipsen et al. (2,3) based on the 1,2-dipalmitoyl-*sn*-glycero-3-phosphocholine (DPPC)-cholesterol phase diagram determined by deuterium NMR and DSC (4). Investigations of phosphatidylcholine (PC)-cholesterol phase diagrams for a number of saturated and monounsaturated PC species including DPPC, 1-stearoyl-2-elaidoyl-*sn*-glycero-3-phosphocholine (SEPC), 1-palmitoyl-2-petrosenoyl-*sn*-glycero-3-phosphocholine (PPetPc) (5,6), and 1-palmitoyl-2-oleoyl-*sn*-glycero-3-phosphocholine (POPC) (7) indicated that the cholesterol-PC phase diagram is very similar for all PCs, but phase transition temperatures depend on lipid hydrocarbon chain length and degree of unsaturation. In the cholesterol-containing lipid mixtures three different lamellar phases, liquid disordered, l_d, solid ordered, s_o, and liquid ordered, l_o, were identified.

The liquid-disordered state is characterized by rapid *gauche*/*trans* isomerization of lipid hydrocarbon chains and a distinct order parameter profile with high order from the carbonyl group to the middle of the chain and rapid order decrease to the terminal methyl group (8,9). Chain segments perform librational motions with correlation times of picoseconds, *gauche*/*trans* isomerization with correlation times in the 100 ps range, rapid lipid rotational diffusion about the bilayer normal with correlation times of ~1 ns (10), collective motions with correlation times from nano- to microseconds (11), and lateral diffusion at rates of the order of 10^{-11} m^{2}s^{-1} (12–14).

In contrast, in the solid-ordered state lipid hydrocarbon chains are packed in a crystalline lattice, *gauche*/*trans* isomerization is mostly suppressed, lipid diffusional rotation about the bilayer normal is very slow (15), and lateral diffusion is lower by orders of magnitude compared to the liquid-disordered state (16,17).

High concentrations of cholesterol in the membranes generate a liquid-ordered state with high chain order in the order parameter plateau region (18). In infrared and NMR experiments conducted on DPPC with specifically deuterated hydrocarbon chains, it was detected that cholesterol strongly hinders *gauche* rotamer formation at carbons C4 and C6 of the chains but much less at carbon C12 (19,20). This appears to be related to the preferred location of cholesterol in the hydrocarbon chain region near the headgroup as found in x-ray experiments conducted on equimolar mixtures of bovine brain sphingomyelin and cholesterol (21). By quasielastic neutron scattering on DPPC-cholesterol mixtures, it was detected that the short alkyl chain of the cholesterol molecules may cross the bilayer midplane at high frequency (22). Changes of the rate of lipid rotational diffusion about the bilayer normal are small (23), and the reduction of lateral diffusion rates is modest (24–26).

Fluorescence microscopy studies conducted on giant unilamellar liposomes with a lipid composition that models

Submitted July 10, 2005, and accepted for publication November 23, 2005.

Address reprint requests to Klaus Gawrisch, NIAAA, NIH, 5625 Fishers Ln., Rm. 3N-07, Bethesda, MD 20892-9410. Tel.: 301-594-3750; Fax: 301-594-0035; E-mail: gawrisch@helix.nih.gov.

0006-3495/06/03/2051/11 $2.00

doi: 10.1529/biophysj.105.070441

the outer monolayer of raft-forming plasma membranes indicated formation of micrometer-size liquid-ordered domains in a liquid-disordered matrix (27–33). Recently it was argued that formation of the l_o phase is a progressive accumulation of randomly distributed sphingomyelin-cholesterol condensed complexes with a short lifetime (34,35). Indeed, rafts in real biological membranes appear to be of submicrometer dimensions (29,36–38), making their detection very difficult.

Another common approach to raft detection is the search for detergent-resistant membrane domains (39). Interpretation of results from triton solubilization studies, typically conducted at a temperature of 4°C, is hotly debated. Evidence was presented that unfavorable interactions between the detergent Triton, sphingomyelin, and cholesterol could drive the formation of domains that may not exist at physiological conditions (40–42). Thus there is a profound need to develop noninvasive tools that detect very small rafts at physiological temperatures in model as well as biological membranes.

Solid-state ^{2}H NMR measurements on deuterated lipids have played an important role in establishing the PC-cholesterol phase diagrams. Coexistence of s_o and l_o phases is identified unambiguously from the distinct differences in the ^{2}H NMR spectra of both phases. However, in most cases coexistence of l_d and l_o phases was only visible as broadening of resonance peaks resulting in a loss of resolution (4,5,7,43). In contrast, electron spin resonance (ESR) spectra of spin labeled lipids recorded in the phase coexistence range showed superposition of signals from l_o and l_d phases (44). The difference between NMR and ESR could be related to the three orders of magnitude longer timescale of ^{2}H NMR in combination with small domain size. Most likely, in the NMR experiments lipids are in a medium rate of exchange between l_d and l_o, which yields broadened spectra. The much shorter timescale of the ESR experiment yields spectra that are a superposition of l_d and l_o resonances.

Ideally, experiments on l_o domain detection should be conducted using noninvasive tools, applicable to both model and biological membranes. The method should be able to detect domains of any size without the need for labeling. Here we explored if magic angle spinning (MAS) ^{1}H NMR meets those criteria. Historically, application of ^{1}H NMR to lipid bilayers was limited by low spectral resolution due to anisotropic proton-proton dipolar interactions (45,46). For fluid lipid bilayers the broadening is mostly from superposition of spectra of bilayers with different orientation to the outer magnetic field. Such inhomogeneously broadened spectra convert into a well-resolved spinning centerband and sidebands at MAS frequencies of a few kilohertz (47,48). Recently we demonstrated that ^{1}H MAS NMR reflects l_d-s_o phase coexistence as superposition of the well-resolved resonances of the l_d phase and the very broad resonances of the s_o phase (49). In this work we explored if coexistence of l_d and l_o phases can be detected as well.

The influence of cholesterol on appearance of lipid ^{1}H MAS spectra of 1,2-dimyristoyl-*sn*-glycero-3-phosphocholine (DMPC) was investigated previously by Forbes et al. (48). At a MAS frequency of 2.6 kHz, an intensity decrease of the chain methylene resonance at 1.3 ppm in the MAS centerband was observed after cholesterol addition. The authors related it to the cholesterol-induced increase of chain order parameters in DMPC. Higher order redistributed intensity from the spinning centerband to sidebands.

We studied the influence of cholesterol addition to several phosphocholines at a much higher MAS frequency of 10 kHz. We started with ^{1}H NMR 1-stearoyl-2-oleoyl-*sn*-glycero-3-phosphocholine (SOPC), a biologically relevant phospholipid that has a main phase transition temperature of 6°C. Interactions of SOPC with cholesterol were studied previously (50–52), but no detailed phase diagram was available (53). We determined the SOPC-cholesterol phase diagram by ^{2}H NMR and ^{1}HHH MAS NMR and observed distinct difference between the MAS NMR spectra of l_d, l_o, and s_o phases. Using ^{1}H dipolar echo NMR spectroscopy (54,55), we linked the spectral differences between l_o and l_d chain methylene resonances quantitatively to differences in the effective strength of proton dipole-dipole interactions between neighbored methylene groups.

The generality of this observation was confirmed in experiments on DPPC for which the phase diagram was previously reported. Similar to natural sphingomyelin this lipid has a main phase transition temperature of 41°C. At a cholesterol concentration and temperature that corresponded to a high concentration of l_o, we detected not only the previously reported redistribution of signal intensity from spinning center- to sidebands but also a substantial increase in resonance linewidth.

Finally we conducted experiments on a ternary mixture of DPPC/DOPC (1:1, mol/mol) with 30 mol % cholesterol that models the outer monolayer of raft-forming plasma membranes (43). We observed that the onset of the l_o/l_d phase coexistence is easily detected as linebroadening/decrease of signal intensity of the chain methylene resonance at 1.3 ppm, recorded as a function of temperature. At a temperature near the onset of l_o phase formation, resonances were homogenously broadened; but at sufficiently low temperature, the l_o domains did grow sufficiently large in size that spectra are a superposition of l_o and l_d states. The phase boundaries and the l_o phase content determined by MAS ^{1}H NMR agreed well with the fluorescence microscopy data for giant unilamellar vesicles of the same lipid composition.

MATERIALS AND METHODS

SOPC, 1-stearoyl$_{d35}$-2-oleoyl-*sn*-glycero-3-phosphocholine (SOPC-d35), 1,2-dioleoyl-*sn*-glycero-3-phosphocholine (DOPC), and DPPC were purchased from Avanti Polar Lipids (Alabaster, AL). Cholesterol was purchased from Sigma-Aldrich (St. Louis, MO). Deuterium-depleted water and ^2H_2O were purchased from Cambridge Isotope Laboratories (Woburn,

MA). Multilamellar vesicles were prepared by hydration of a lipid film with excess buffer (10 mM piperazine-*N*,*N*′-bis(2-ethanesulfonic acid) (PIPES)), pH 7.4, 100 mM NaCl, and 50 μM diethylenetriaminepentaacetic acid (DTPA) followed by freeze-thaw cycles for proper equilibration. For proton NMR experiments, samples were prepared using ^2H_2O. Multilamellar vesicles were concentrated and separated from extra buffer by centrifugation. From 2 to 4 mg of lipid were transferred to a 4 mm Zirconia rotor fitted with Kel-F inserts generating a spherical sample volume of 11 μL (Bruker Spectrospin, Billerica, MA).

NMR measurement

^{1}H MAS NMR

MAS NMR experiments were carried out on a Bruker DMX500 spectrometer equipped with a wide bore 11.7 Tesla magnet, a BVT-2000 variable temperature accessory, a MAS control unit, and a triple resonance variable temperature cross-polarization MAS probe for 4-mm rotors (Bruker Instruments, Billerica, MA). ^{1}H NMR experiments were carried out at a resonance frequency of 500.13 MHz using a spectral width of 25 kHz, which included the spinning centerband and one or two orders of sidebands, depending on the spinning frequency, 10 or 5 kHz, respectively.

The temperature was calibrated by measuring the chemical shift difference between water and choline in a micellar sample of 1,2-dicaproyl-*sn*-glycero-3-phosphocholine (Avanti Polar Lipids, Alabaster, AL) loaded into an identical 11-μL insert for 4-mm MAS rotors as above. The chemical shift as a function of temperature was measured on the same sample in a 5-mm tube in a high resolution probe whose temperature had been calibrated to $\pm$0.1°C with a thermocouple. We chose a MAS frequency of 10 kHz as a compromise between acceptable spectral resolution of l_o phase spectra and reliable temperature control with temperature gradients across the sample of $<$3°C (49). MAS does not affect lipid bilayers except for mild dehydration that depends on the difference between water and membrane density (56,57).

The probe was tuned and matched to the resonance frequency at a temperature corresponding to the midpoint of the investigated temperature range (10°C for SOPC-cholesterol samples and at 20°C for DOPC/DPPC/cholesterol samples). The maximum decrease of signal intensity due to probe mismatch and/or a temperature dependence of the probe Q-factor was $<$5% over the entire investigated temperature range.

^{2}H NMR

^{2}H NMR experiments were performed on a Bruker DMX300 wide-bore spectrometer at 46.1 MHz. Spectra were acquired using the quadrupolar echo pulse sequence (d_1-90°$_x$-τ-90°$_y$-acquire) with a repetition time $d_1 = 0.3$ s, a 2.7-μs 90° pulse, a 50-μs delay between pulses, and a spectral width of 200 kHz. The carrier frequency was placed exactly at the center of the spectrum. The free induction decay was left-shifted with a resolution of 1/10th of a dwell time unit to ensure that the first time point of the data set used in Fourier transformation corresponded exactly to the echo maximum. This avoids first order phase correction of the spectra and the related distortions of the spectral baseline. The phase transitions of lipids were followed by the shape change of the ^{2}H NMR spectra or by the plot of the first spectral moment, M_1, calculated according to

$$M_1 = \int_0^\infty \omega f(\omega) d\omega \Big/ \int_0^\infty f(\omega) d\omega,$$

where the integration limit $\omega = 0$ corresponds to the center of the symmetric spectra.

^{1}H NMR dipolar echo spectroscopy

The utilization of dipolar echo experiments to measure the interpair second moment, M_{2i}^{ip}, the contribution to proton dipole-dipole interaction from protons in adjacent methylene groups, was shown previously (54,55,58). Briefly, experiments were conducted on a Bruker DMX300 spectrometer at 300.1 MHz using a solids probe with a solenoidal sample coil. The dipolar echo was acquired using the pulse sequence ($d_1 - 90°_x - \tau - 90°_y$-acquire) with a repetition time $d_1 = 10$ s and a 4-μs 90° pulse. The delay time τ was varied from 5 to 500 μs. For data analysis the logarithm of the echo amplitude was plotted versus τ^2 and the resulting decay approximated by a superposition of exponentially decaying functions. It was shown earlier that the decay of the echo amplitude can be approximated with good precision as

$$E(\tau) = \sum_i n_i \exp(-1/2\gamma^2 M_{2i}^{ip} \tau^2), \quad (1)$$

where summation is over protons, n_i, of lipid segments with different interpair second moments, M_{2i}^{ip}, and γ is the gyromagnetic ratio of protons. Typically values of M_{2i}^{ip} are grouped into NMR signals from regions of high, medium, and low lipid order. We could only determine M_{2i}^{ip} of the lipid region with the highest order, corresponding to the lipid glycerol group and the hydrocarbon chain segments corresponding to the chain order parameter plateau (55).

RESULTS

Proton MAS NMR of SOPC-cholesterol mixtures

As previously reported, SOPC spectra in the l_d phase converted from very broad to well resolved at moderate MAS frequencies of 2–3 kHz (49). The linewidth at half-height was in the range of 10–50 Hz. The resonances in the centerband were flanked by a series of spinning sidebands spaced at multiples of the spinning frequency. The chemical shifts of resonances were close to chemical shifts in organic solvents, which eased signal assignment (Table 1). With increasing MAS frequency, the spectral intensity redistributed from sidebands toward the centerband. For SOPC in the l_d phase at 25°C and a MAS frequency of 10 kHz, 99% of total signal intensity was in the centerband, permitting us to relate centerband integral resonance intensities directly to the number of contributing protons (Table 1).

TABLE 1 SOPC ^{1}H MAS NMR resonances assignment and comparison of spectral integral intensity measured at 25°C at a MAS frequency of 10 kHz with the number of protons per resonance

		Peak integral intensity	
Peak assignment	Peak position, ppm	Theory	Measured
-CH_3	0.88	6	6.58
$(CH_2)_n$	1.3	48	45.5
$\underline{CH_2}$-CH_2-CO	1.6	4	4.24
$\underline{CH_2}$-CH=CH-$\underline{CH_2}$	2.05	4	4.01
CH_2-CO	2.3–2.4	4	3.93
$N(CH_3)_3$ or $\underline{CH_2}$-NH_3	3.28	9	9.02
$\underline{CH_2}$-$N(CH_3)_3$	3.68	2	1.99
CH_2-OP (glycerol)	4.05	2	1.82
PO-CH_2 (choline)	4.3	2	3.05*
OCO-CH_2 (glycerol)	4.2	1	3.05*
	4.44	1	0.98
-CH=CH- and OCO-CH in glycerol	5.3	3	3

*Superimposed.

For SOPC-cholesterol mixtures spectral changes with decreasing temperature and increasing cholesterol content were more complex due to l_o phase formation and fast exchange of lipids between l_d and l_o phases. At higher temperatures, the broadening of SOPC centerband resonances with increasing cholesterol concentration was insignificant (Fig. 1 *A*). In particular, at 37°C addition of 15 mol % cholesterol broadened the chain methylene resonance at 1.3 ppm by 5–10 Hz and addition of 30 mol % cholesterol by 10–15 Hz. The cholesterol resonances were visible in the spectral centerband as broad peaks at the base of lipid peaks in the 0.6–1.8 ppm range. The cholesterol-induced increase in acyl chain order of SOPC was reflected as intensity increase of MAS sidebands (Fig. 1 *A*, *inset*).

At lower temperatures and cholesterol concentrations of 15 mol % and higher, we observed a temperature-dependent decrease of SOPC signal height over a wide temperature range (Figs. 1, *B* and *C*, and 2 *A*). The changes in lineshape of the choline resonance at 3.25 ppm as well as other headgroup and glycerol resonances in the spectral range from 3.6 to 4.6 ppm could be reasonably well approximated as superposition of broad and narrow spectra as is evidenced by the presence of isosbestic points in the superimposed spectra. In contrast, the chain methylene resonance at 1.3 ppm displayed a narrow component with a linewidth that increased from ~50 to 150 Hz over the temperature range from 45°C to 6°C and a superimposed broad component with a linewidth of a 1,000 Hz that appeared toward the low temperature end of the transition. Before the transition midpoint, the signal height of the narrow component decreased primarily because of signal broadening, whereas below the transition midpoint signal intensity loss was primarily due to appearance of a superimposed, kHz-wide resonance. The resulting non-Lorentzian line shape is visible both in spinning center- and sidebands (Fig. 1 *C*).

The temperature-dependent spectral changes above are in agreement with expectations based on the general appearance of PC-cholesterol phase diagrams (2,5). Let us discuss appearance of chain methylene resonances first. At sufficiently high cholesterol content, published phase diagrams indicate that the mixture changes from pure l_d to an l_d-l_o phase coexistence and then to an l_o-s_o coexistence as temperature is lowered. According to ^{2}H NMR, the domains in the l_d-l_o coexistence are in a size range that yields spectra that are broadened by medium rate exchange of lipids between phases (vide infra). Because the differences in ^{1}H NMR resonance linewidth between spectra of l_d and l_o phases are somewhat smaller than the differences in ^{2}H NMR quadrupolar splittings, the ^{1}H MAS NMR spectra of SOPC with l_d-l_o exchange are likely to be in the range of fast exchange. Therefore resonances are expected to be homogenously broadened, with a linewidth that increases with increasing l_o content, as it was observed. Over the phase transition, with decreasing temperature the l_d phase disappears and s_o appears. Lipids in the s_o phase are in slow

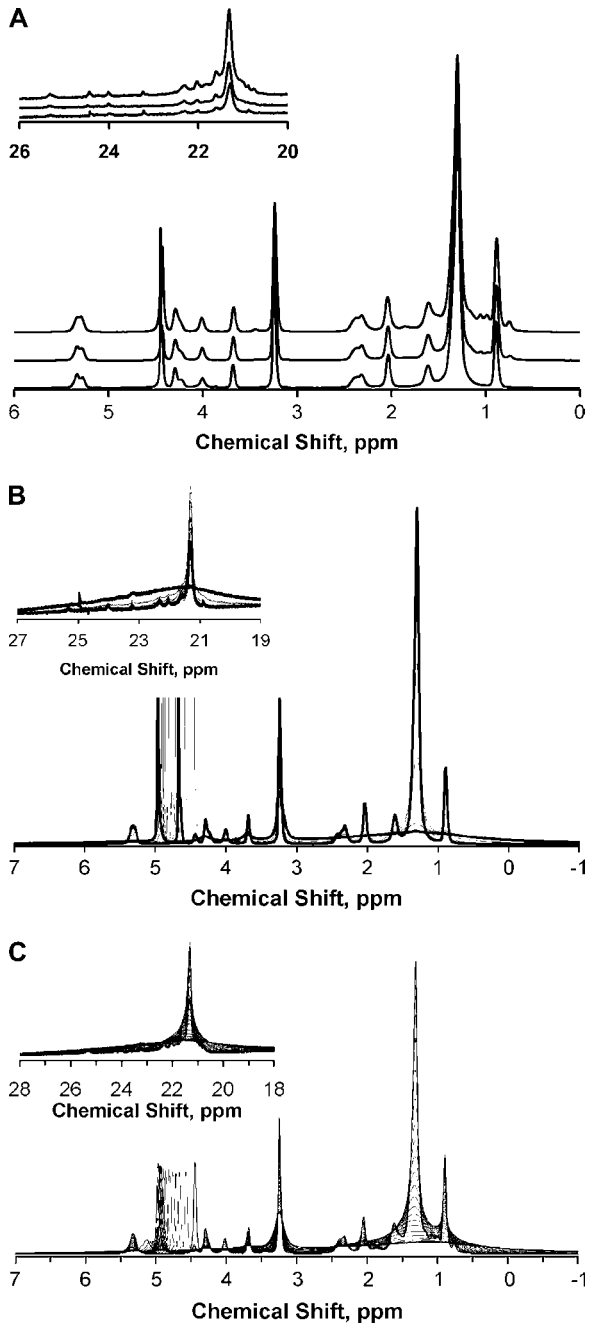

FIGURE 1 (*A*) Spectra of SOPC, SOPC/cholesterol 85:15 mol %, and SOPC/cholesterol 70:30 mol % at 37°C. The first order spinning sidebands are shown in the inset with 20-fold magnification. (*B*) Temperature-dependent changes of 10 kHz ^{1}H MAS NMR spectra of SOPC multilamellar vesicles. Superimposed spectra are shown to emphasize the presence of isosbestic points in the course of the gel-to-liquid crystalline phase transition. Bold lines show spectra taken at the highest (37°C) and at the lowest (2°C) temperatures. The first order spinning sidebands are shown in the inset with 20-fold magnification. (*C*) Temperature-dependent changes of 10 kHz ^{1}H MAS NMR spectra of SOPC/cholesterol 70:30 multilamellar vesicles. Superimposed spectra are shown to emphasize the presence of isosbestic points in the phase coexistence region. Bold lines show spectra taken at the highest (37°C) and at the lowest (2°C) temperatures. The first order spinning sidebands are shown in the inset with 20-fold magnification.

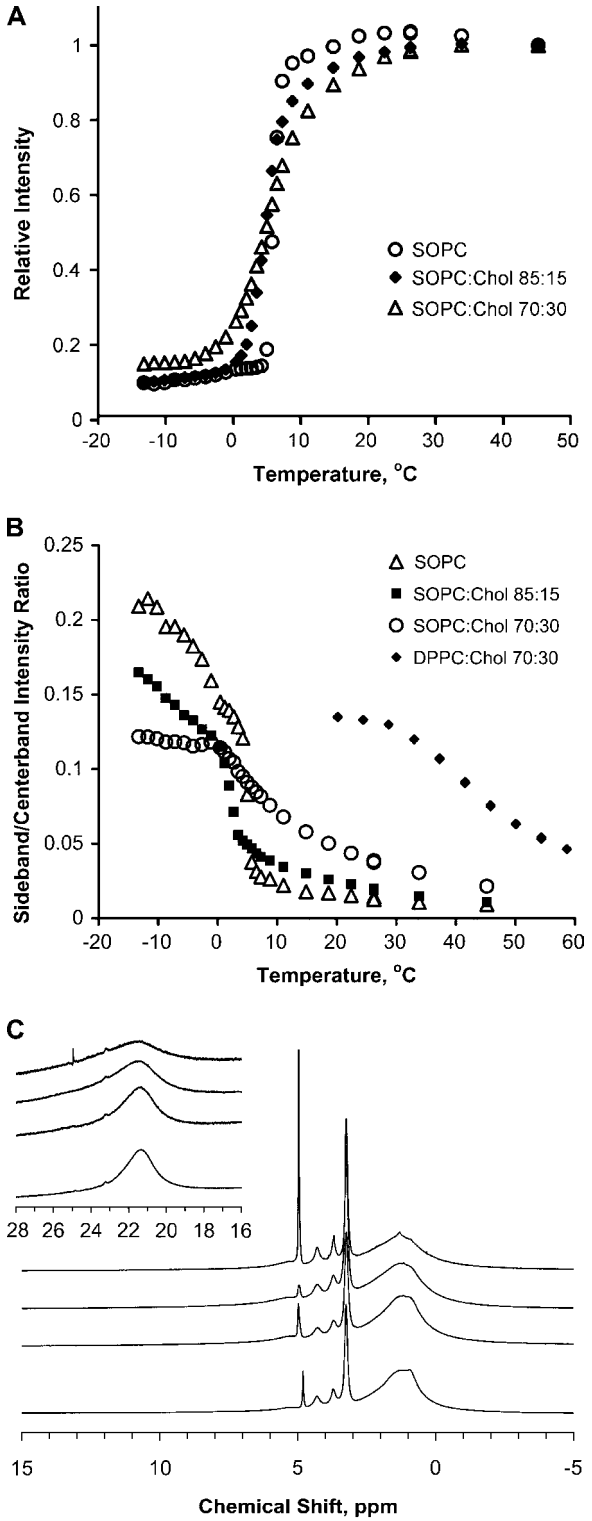

FIGURE 2 (*A*) Temperature dependence of the methylene resonance intensity at 1.3 ppm in the spinning centerband for SOPC, SOPC/cholesterol 85:15 mol %, and SOPC/cholesterol 70:30 mol %. (*B*) Plot of the first spinning sideband/centerband intensity ratio for SOPC, SOPC/cholesterol 85:15 mol %, SOPC/cholesterol 70:30 mol %, and DPPC/cholesterol 70:30. (*C*) ^{1}H MAS NMR spectra of SOPC, SOPC/cholesterol 85:15 mol %, SOPC/cholesterol 70:30 mol %, and DPPC/cholesterol 70:30 (from *top* to *bottom*) at the low temperature end of the transition at 4°C, −2°C, −4°C, and 35°C, respectively. The first order spinning sidebands are shown in the inset with 20-fold magnification. The SOPC spectrum corresponds to the s_o phase; SOPC/cholesterol 85:15 mol % represents coexistence of s_o and l_o, and SOPC/cholesterol 70:30 mol % is mostly the l_o phase.

exchange with l_o and l_d. They are seen as a kHz-wide resonance that is superimposed on the homogeneously broadened signal of the combined signal of l_d and l_o phases.

Signal broadening of glycerol and headgroup resonances upon transition from l_d to l_d-l_o phase coexistence is much smaller than for the chain methylene protons, and spectral differences are less distinct. At lower temperatures the broader resonances of lipids in the s_o phase are superimposed. Choline headgroup signals are similar in l_o and s_o phases but are sensitive to headgroup dehydration (49).

Appearance of ^{1}H MAS spectra is in agreement with calorimetric measurements on SOPC-cholesterol mixtures (50,51). By calorimetry two partially superimposed transitions were identified, a broad transition at higher temperature, which has been tentatively assigned to entering l_d-l_o phase coexistence and a narrower transition at lower temperature most likely related to s_o phase formation. The temperatures of both DSC transitions agree with the temperature ranges of spectral changes in the proton MAS NMR spectra.

^{2}H NMR experiments on SOPC-d_{35}-cholesterol

The onset of s_o phase formation is more conveniently detected by ^{2}H NMR experiments on SOPC-d_{35} with a perdeuterated stearic acid chain. Characteristic spectra of SOPC-d_{35}-cholesterol mixtures as a function of temperature are shown in Fig. 3. The formation of the s_o phase is reflected by appearance of the much broader s_o resonance that is superimposed on the narrower spectrum from liquid phases. The transition is also visible as a discontinuity in the plot of the first spectral moment, M_1, versus temperature (Fig. 3 *C*).

The midpoint of the l_d-s_o phase transition of plain SOPC-d_{35} bilayers was at 3.5°C ± 0.5°C. Addition of 15% cholesterol significantly increased lipid quadrupolar splittings of the l_o phase, decreased the temperature at which the s_o phase appeared to 2.0°C ± 0.5°C, and broadened the transition. The molar ratio of SOPC-d_{35} in l_o and s_o phases was determined by spectral analysis as described earlier (4,59,60). Briefly, a judiciously determined fraction of the spectrum obtained at the higher cholesterol concentration that is enriched in l_o is subtracted from the spectrum at lower cholesterol content to yield the spectrum of a pure s_o phase. The upper and lower sterol concentrations at which pure s_o and l_o states are formed are then calculated by the lever rule from the fractional intensities of superimposed l_o and s_o spectra. We applied this approach to the spectra of SOPC-d_{35}-cholesterol mixtures at molar ratios 85:15 and 70:30 and obtained phase boundaries at cholesterol concentrations of 7–9% for the transition from the s_o phase to s_o/l_o phase

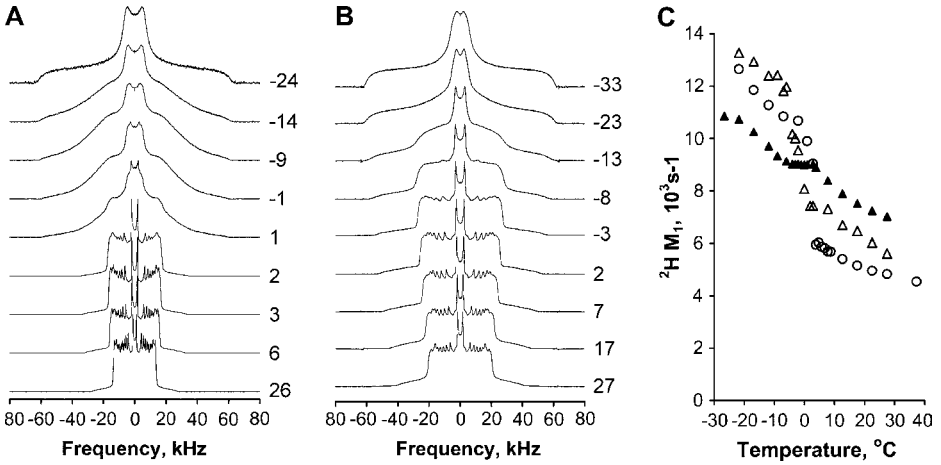

FIGURE 3 (*A*) Deuterium NMR spectra of SOPC-d_{35} recorded at −24°C, −14°C, −9°C, −1°C, 1°C, 2°C, 3°C, 6°C, and 26°C. (*B*) Deuterium NMR spectra SOPC-d_{35}/cholesterol 70:30 mol % recorded at −33°C, −23°C, −13°C, −8°C, −3°C, 2°C, 7°C, 17°C, and 27°C. (*C*) Temperature dependence of first moments, M_1, of deuterium NMR spectra of SOPC-d_{35} (○), SOPC-d_{35}/cholesterol 85:15 (△), and SOPC-d_{35}/cholesterol 70:3 (▲).

coexistence and 35–38% for the transition from s_o/l_o to a single l_o phase (Fig. 4). The spectral subtraction procedure worked reliably over the temperature range from −2°C to −11°C. Due to temperature-dependent changes in the spectra of l_o and s_o phases, the distinction between the phases at lower temperatures became uncertain. Previously those temperature-dependent changes were related to a continuous slowdown of diffusive axial rotation of lipids (15,61,62).

Deuteration of the *sn*-1 chain lowered the l_d-s_o phase transition of pure SOPC by 2.5 degrees. To be able to combine results of ^{1}H MAS NMR and ^{2}H NMR experiments in one phase diagram, we also recorded the ^{1}H MAS NMR spectra of the SOPC-d_{35}/cholesterol mixture 70:30 mol % as a function of temperature. The phase behavior of the deuterated SOPC-cholesterol was indistinguishable from protonated SOPC-cholesterol after adding 3°C to all phase transition temperatures.

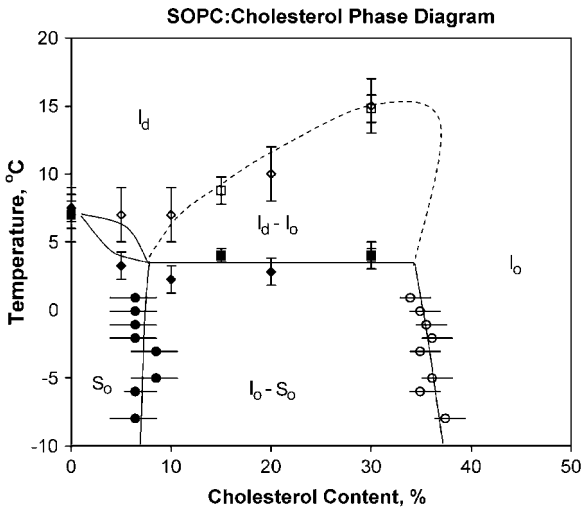

FIGURE 4 Schematic phase diagram of a SOPC-cholesterol binary mixture as discussed in the text. The lines connecting the points are guides to the eye. The following points were determined from DSC data (♦, onset; ◇, completion of the phase transition) (43), from proton MAS NMR (■, onset; □, completion), and from deuterium NMR (●, ○). Phase transition temperatures measured by ^{2}H NMR on *sn*-1 chain deuterated SOPC were raised by 3°C to compensate for the difference in phase transition temperatures between deuterated and protonated lipids.

SOPC-cholesterol phase diagram

The SOPC-cholesterol results presented above are consistent with the phase diagram shown in Fig. 4. The onset of the decay ^{1}H MAS NMR intensity of the methylene signal of hydrocarbon chains at 1.3 ppm correlated well with the onset of the high temperature transition seen by DSC (50). According to the phase diagram this is a transition from the l_d phase to the l_d-l_o phase coexistence. The dashed line on the phase diagram represents the boundary of the l_d-l_o phase coexistence region. Because of the low number of experimental data points, this boundary is only a visual guide. The Gibbs phase rule applied to a binary lipid mixture predicts that coexistence of l_d, l_o, and s_o phases can only be observed at one specific temperature (3°C) in the phase diagram. At lower temperatures the spectra of SOPC/cholesterol 85:15 mol % and 70:30 mol % correspond to coexistence of l_o and s_o phases and at higher temperature to coexistence of l_d and l_o. Our results provide strong evidence for this phase diagram at temperatures below −2°C but could be consistent with other diagrams that do not show immiscibility of l_o and l_d phases at high temperature.

Based on the SOPC-cholesterol phase diagram it is feasible to determine the SOPC spectra of pure l_d, l_o, and s_o states (Figs. 1 *A* and 2 *B*). At 30 mol % cholesterol in SOPC in the mixture, the l_o phase content is 85–90% at low temperature. Therefore the spectrum of the SOPC/cholesterol 70:30 mol % mixture below 3°C is very close to the spectrum of a pure liquid-ordered phase (Fig. 2 *C*). Spectra of the pure l_d phase are detected at sufficiently high temperature, and spectra of the pure s_o phase are detected at low temperature and low cholesterol content. There are distinct differences in the linewidth of the methylene proton resonance

of hydrocarbon chains at 1.3 ppm between the l_d phase, 50–100 Hz, the l_o phase, 500 Hz to 1 kHz, and the s_o phase, 1–3 kHz (Fig. 2 *C*).

The temperature-dependent changes in the ^{1}H MAS NMR spectra of the SOPC/cholesterol70:30 mol % sample reflect the onset of the l_o phase in the membrane as temperature is lowered. Although this transition is very well detected in the ^{1}H MAS spectra as significant broadening of the 1.3 ppm resonance, the ^{2}H NMR spectra of the deuterated lipid do not show a distinct discontinuity. In contrast, appearance of the s_o phase resulted in large spectral changes in the ^{2}H NMR spectra (M_1, Fig. 3 *C*), whereas the ^{1}H MAS NMR spectra showed only additional broadening that was difficult to distinguish from the already broadened resonances of the l_o phase.

The appearance of a gel phase is detected in the ^{1}H MAS spectra as well by following the intensity ratio of center- to sideband intensity (I_c/I_s) of chain methylene resonances. The chain order parameters in the s_o phase are much higher, resulting in a lower I_c/I_s ratio. The discontinuity in the plot of the I_c/I_s versus temperature is a sensitive measure for appearance of the s_o phase, as seen in the spectra of the SOPC/cholesterol 85:15 mol % mixture (Fig. 2 *B*). The s_o phase content in the 70:30 mol % spectra is very low. Consequently, both the temperature dependence of the I_s/I_c ratio of the ^{1}H MAS NMR and the M_1 temperature dependence of the ^{2}H NMR spectra do not show a distinct discontinuity.

How general are the spectral characteristics of the l_o phase in ^{1}H MAS NMR spectra? To address this question we studied a DPPC/cholesterol 70:30 mol % mixture that is in the l_o phase according to the phase diagram reported by Vist and Davis (4). After correction for the difference in phospholipid phase transition of temperatures (41°C vs. 6°C), the spectra of the DPPC-cholesterol (Fig. 2 *C*, the *bottom spectrum*) and SOPC-cholesterol mixtures are very similar. The temperature dependence of the I_s/I_c intensity ratio of the DPPC/cholesterol 70:30 mol % also resembles behavior of the SOPC/cholesterol 70:30 mol % mixture (Fig. 2 *B*).

^{1}H-^{1}H interpair dipolar interactions

MAS is capable of averaging spatial anisotropic tensors with axial symmetry, e.g., the ^{1}H-^{1}H dipole-dipole interaction between the two protons in a methylene group. The resulting ^{1}H MAS spectra have excellent resolution in the spectral centerband. However, those favorable tensor properties may get lost when strong fluctuating ''interpair'' dipolar interactions from protons of neighbored methylene groups are superimposed on intrapair dipolar couplings. It was investigated if the transition to the l_o phase is related to an increase of interpair dipolar interactions.

In dipolar echo spectroscopy (54,58) stronger interpair dipolar interactions result in a faster echo decay. For lipids in the s_o phase the echo decay is a superposition of a fast decay arising from sections of the aliphatic chains and the glycerol and a slower decay from the polar headgroups (55). The interpair dipolar interactions in the l_d phase are strongly reduced due to rapid *gauche/trans* isomerization of hydrocarbon chains resulting in a much slower decay of dipolar echo amplitudes. Also fewer protons contribute to the lipid regions of highest interpair moment, seen as a decrease of fractional intensity of fastest decay.

We studied the dipolar echo decay for plain SOPC and the SOPC/cholesterol, 70:30 mol % mixture above and below the phase transition temperature (Fig. 5) to determine if the interpair moment increases with l_o phase formation. Experimental values of highest M_{2i}^{ip} were compared with calculated values. A rigid hydrocarbon chain in all-*trans* conformation that performs rapid diffusional motions about its long axis

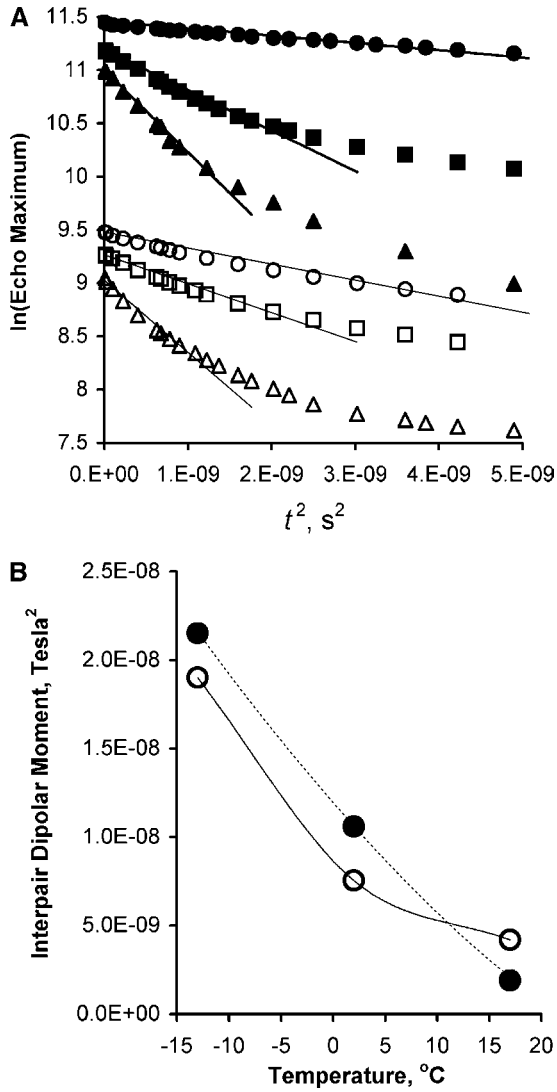

FIGURE 5 (*A*) Delay time dependence of the dipolar echo maximum for SOPC (*solid symbols*) and SOPC-d_{35}/cholesterol 70:30 (*open symbols*), measured at temperatures of 17°C (*circles*), 4°C, and −13°C (*triangles*). The curves were shifted along the *y* axis to reduce overlap. (*B*) Interpair dipolar moments determined from the slope of curves at short delay times as shown in panel *A*.

has an interpair moment of $2.32 \times 10^{-8}\ T^2$ (55). At low temperatures the highest M_{2i}^{ip} values for both SOPC and SOPC/cholesterol 70:30 mol % samples are slightly lower than the values calculated for a chain in all-*trans* configuration. Therefore, in both the l_o and s_o phase, the probability of *gauche*/*trans* isomerization of lipid acyl chains is very much reduced. In addition to an increase in the strength of interpair interactions, we also observed an increase in the number of lipid protons in the membrane regions with highest interpair moments. This suggests that fluctuating, strong dipolar interactions between neighbored methylene groups of hydrocarbon chains are responsible for the substantial increase of linewidth of chain l_o phase resonances in the ^{1}H MAS NMR spectra.

DOPC/DPPC/cholesterol

The results above suggested that ^{1}H MAS NMR is a powerful method for detection of l_d-l_o phase coexistence. We tested this proposition by investigating a DOPC/DPPC 1:1 mixture containing 30% cholesterol for which l_d-l_o phase coexistence had been detected previously by fluorescence microscopy on giant unilamellar liposomes (28,42). In the fluorescence experiments, ordered states (l_o and s_o) were associated with domains that appeared dark in the fluorescent microscope because of exclusion of fluorescent dye. The regions of l_d phase contained higher concentrations of the fluorescence dye and are brighter. The circular shape of dark ordered domains allowed their assignment as l_o (28,30), which was also confirmed by deuterium NMR (43).

It was reported that upon lowering temperature, the mixture converted from l_d to l_d-l_o phase coexistence at 30°C. With decreasing temperature, the l_o domains grew in size until they covered 50% of the membrane surface at 10°C (Fig. 6 *B*). We detected a significant increase in linewidth of lipid resonances in the ^{1}H MAS NMR spectra that coincided with the appearance of the l_o phase (Fig. 6 *A*). The bold spectra were recorded at 45°C and 8°C, the highest and lowest temperatures, respectively. The superimposed spectra displayed a series of isosbestic points indicating superposition of spectra from two states. However, some deviations from isosbestic behavior were observed in the spectral range covering the chain methylene resonances 0.5–2.5 ppm at the onset of broadening near 30°C. The latter agrees with observations from ^{2}H NMR experiments that were published earlier (43). According to those results, the l_o phase domains at temperatures near 30°C are sufficiently small to result in intermediate exchange of lipid molecules between l_o and l_d phases on the NMR timescale. Nevertheless, the onset of l_o phase formation is easily detected in the plot of the 1.3 ppm signal versus temperature, which has a distinct break point at 30°C.

The amount of l_o and l_d phase at 8°C was determined by subtraction of a judiciously determined fraction of the high temperature spectrum recorded at 45°C, representing the l_d phase. To compensate for the minor temperature dependence of l_d phase spectra, the free induction decay was multiplied with an exponential window function corresponding to a spectral broadening of 100 Hz. The criterion for proper subtraction was appearance of the difference spectrum (Fig. 6 *A*, *bottom panel*). Subtracting too much l_d phase intensity resulted in negative spikes, whereas subtracting too little produced positive spikes. The spectrum of the pure l_o state, obtained by subtraction of 35% l_d phase intensity, is shown as a bold line in the bottom panel of Fig. 6 *A*. At 8°C 33 ± 7% of the lipids were in l_o phase. We used this subtraction approach to determine the fraction of phospholipids in l_d and l_o phases as a function of temperature and compared it with the l_d and l_o phase fractions determined from the area estimates in fluorescence microscopy studies (Fig. 6 *B*). There is a reasonable agreement, especially with regard to the onset

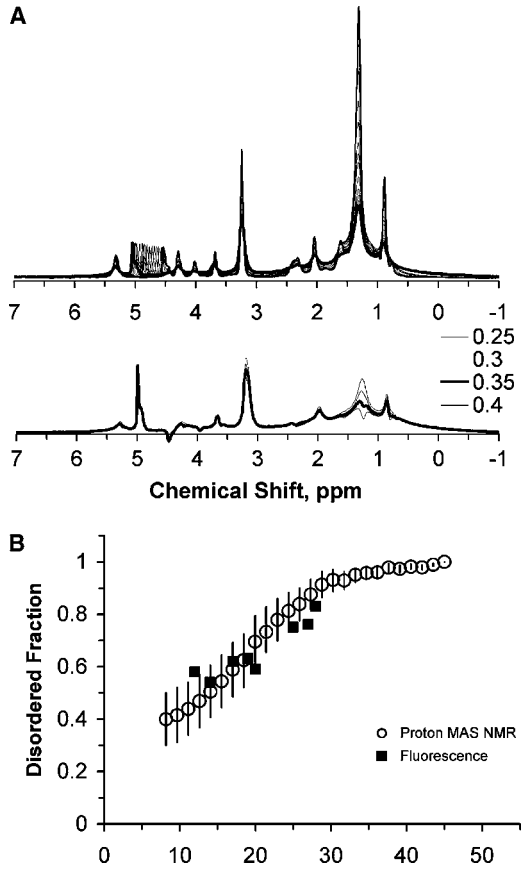

FIGURE 6 (*A*) The top panel shows the superimposed ^{1}H MAS NMR spectra of DOPC/DPPC 1:1 30 mol % cholesterol, recorded as a function of temperature. Spectra recorded at the highest (45°C) and the lowest (8°C) temperatures are shown as bold lines. The bottom panel shows the spectrum of the pure l_o phase at 8°C. It was generated by subtraction of a judiciously chosen fraction of the pure l_d phase spectrum, recorded at 45°C. The bold line corresponds to subtraction of 35 mol % of l_d. The thin lines reflect subtraction of smaller or larger amounts of l_d. (*B*) Fraction of lipid in the disordered state as a function of temperature determined from the ^{1}H MAS spectra (○) and the area fraction of disordered domains determined by fluorescence microscopy (■) (S. L. Veatch and S. L. Keller, unpublished).

temperature of l_o formation. It should be noted that there can be a systematic deviation between NMR and fluorescence results because NMR reports fractions of proton resonance intensity of superimposed l_d and l_o resonances, whereas the fluorescence analysis reports fractions of lateral area of l_d and l_o phases. Also, the procedure above does not account for changes in the composition of l_d and l_o phases that may result in minor spectral changes. This is visible for the resonance at 2.05 ppm, which is unique to DOPC. The prominence of the 2.05 ppm resonance after spectral subtraction (Fig. 6 *A bottom*) is indicative for enrichment of the l_d phase with DOPC.

DISCUSSION

It was observed that the ^{1}H MAS NMR spectra of the liquid-disordered, the liquid-ordered, and the solid-ordered phases are distinctly different. At a MAS frequency of 10 kHz, the resonance of hydrocarbon chain methylene protons at 1.3 ppm had a linewidth of ~50Hz in the l_d phase, ~1 kHz in the l_o phase, and several kHz in the s_o phase. By ^{1}H NMR dipolar echo spectroscopy, it was determined that the effective strength of intramolecular ^{1}H-^{1}H dipolar interactions between the protons of adjacent methylene groups increases upon transition to the l_o phase, most likely because of a lower probability of *gauche/trans* isomerization. The resolution of resonances depends on the tensorial properties of ^{1}H-^{1}H dipole-dipole interactions in lipid hydrocarbon chains. If the tensor commutes with itself at all different tensor orientations under MAS sample rotation, then spectra are inhomogeneously broadened and relatively low MAS frequencies are sufficient to convert the spectra into resonances with narrow centerband resonances and spinning sidebands (63,64). Interactions between pairs of protons, like those in a methylene group, fulfill this commutation condition. However, multiproton interactions, like those between adjacent methylene groups, in combination with a low probability of chain isomerization, may result in homogeneous line broadening that is not resolved at modest MAS frequencies.

This linebroadening of chain resonances in the l_o phase took place without apparent reduction of diffusional motions of lipids about the bilayer normal. The ^{2}H NMR spectra of lipid hydrocarbon chains in l_o clearly indicate that lipid rotational diffusion measured on the timescale of 10^{-5} s is still sufficiently fast. This is in clear distinction to the s_o phase where lipid hydrocarbon chains are packed in a crystalline lattice and chain rotational diffusion is drastically reduced. In the s_o phase not only ^{1}H-^{1}H dipole-dipole interactions between neighbored methylene groups of the same hydrocarbon chain but also intermolecular interactions contribute to the dipolar Hamiltonian. The s_o phase spectra are homogenously broadened, and resolution of the ^{1}H MAS resonances is even lower compared to l_o.

The strong linebroadening of chain resonances upon transition of lipids into the l_o phase makes ^{1}H MAS NMR a sensitive tool for detection of l_o-domains, irrespective of their size. Appearance of spectra in mixed phase states depends on the rate of lipid exchange between the domains. When domains are small, lipids may exchange rapidly between l_d and l_o states. In case of rapid exchange, the resonance lines have Lorentzian shape with a linewidth, $\Delta\nu_{1/2}$, that reflects the fractional contributions of ordered and disordered phases

$$\Delta\nu_{1/2} = p_o\Delta\nu^o_{1/2} + p_d\Delta\nu^d_{1/2},$$

where p_o and p_d are the mol fraction of liquid-ordered and -disordered phases, respectively, and $\Delta\nu^o_{1/2}$ and $\Delta\nu^d_{1/2}$ are the linewidth of resonances from those phases. Because the linewidth of chain resonances in l_o is more than one order of magnitude larger compared to l_d, even a small fraction of an l_o phase in exchange with l_d increases $\Delta\nu_{1/2}$significantly and reduces signal height. This is easily detected in a plot of signal intensity versus temperature. The graphs show a distinct break point at the onset of l_o phase formation (Figs. 2 *A* and 6 *B*).

Formation of large domains results in signal superposition of l_d and l_o phase resonances, seen as isosbestic points in superimposed spectra recorded as a function of temperature. The onset of l_o phase formation is initially seen as proportional intensity loss of the l_d resonance. The much broader l_o resonance has very low intensity and becomes visible only after a substantial fraction of lipid has converted to l_o.

The rate of lipid exchange, which determines NMR line shape, depends on domain size, diffusion rates within domains, and the rate of lipid transfer between phase boundaries. Studies on cholesterol-lipid mixtures (24–26) have shown that lipid diffusion rates in l_o are by the factor of 2–3 lower than those of l_d. Recent experiments on lipid diffusion in cholesterol-lipid mixtures conducted with MAS at this laboratory yielded a twofold increase of activation energies of lipid diffusion in the l_d-l_o phase coexistence region but no indications for confinement of lipid diffusion to submicrometer size domains (26). Thus the rate of lipid exchange between l_d and l_o phases depends primarily on domain size and shape.

Crude estimates of domain size are obtained from the condition that NMR resonances convert from homogenous signal broadening to signal superposition due to l_o-l_d exchange (medium rate exchange). This rate is $k \approx \pi(\Delta\nu^o_{1/2} - \Delta\nu^d_{1/2}) \approx \pi\Delta\nu^o_{1/2}$. For simplicity, it is assumed that the domain diameter, d, is twice the distance traveled by diffusion during the time $\tau = 2/k$. With $\Delta\nu^o_{1/2}$= 1 kHz and $D = 5 \times 10^{-8}$cm^2/s, the domain size for medium rate exchange is $d = 2\sqrt{4D\tau} \approx 226$ nm. Formation of smaller domains results in fast exchange and homogenously broadened spectra as observed for l_d-l_o phase coexistence in cholesterol-SOPC mixtures, as well as in DOPC/DPPC 1:1 cholesterol 30% mixture at the onset of l_o domain formation near 30°C. At somewhat lower temperatures, the domains in this mixture became much larger, resulting in signal superposition.

Lipid diffusion rates in the s_o phase are much lower, resulting almost always in slow exchange of lipids between l_o and s_o phases. The ^{1}H MAS NMR spectra are a superposition of resonances from l_o and s_o phases. This is difficult to detect from spectra of chain resonances alone that are broad for both l_o and s_o phases, but the lower center/sideband intensity ratios of chain resonances in l_o are indicators for l_o-s_o phase coexistence.

^{1}H MAS NMR has not only the advantage of detecting l_o phase formation with high sensitivity, it does so without the need for isotopic labeling of lipid constituents. It appears to be feasible to use this method for detection of liquid-ordered and solid-ordered domains not only in model membrane systems but also in biological membranes. The method has very high sensitivity, permitting us to conduct experiments on submilligram quantities of membrane material, including cell membrane preparations and even tissue samples.

REFERENCES

1. Simons, K., and E. Ikonen. 1997. Functional rafts in cell membranes. *Nature*. 387:569–572.
2. Ipsen, J. H., G. Karlström, O. G. Mouritsen, H. Wennerström, and M. J. Zuckermann. 1987. Phase equilibria in the phosphatidylcholine-cholesterol system. *Biochim. Biophys. Acta*. 905:162–172.
3. Ipsen, J. H., O. G. Mouritsen, and M. J. Zuckermann. 1989. Theory of thermal anomalies in the specific heat of lipid bilayers containing cholesterol. *Biophys. J*. 56:661–667.
4. Vist, M. R., and J. H. Davis. 1990. Phase equilibria of cholesterol/dipalmitoylphosphatidylcholine mixtures: ^{2}H nuclear magnetic resonance and differential scanning calorimetry. *Biochemistry*. 29:451–464.
5. Thewalt, J. L., and M. Bloom. 1992. Phosphatidylcholine:cholesterol phase diagrams. *Biophys. J*. 63:1176–1181.
6. Miao, L., M. Nielsen, J. Thewalt, J. H. Ipsen, M. Bloom, M. J. Zuckermann, and O. G. Mouritsen. 2002. From lanosterol to cholesterol: structural evolution and differential effects on lipid bilayers. *Biophys. J*. 82:1429–1444.
7. Bloom, M., and J. L. Thewalt. 1995. Time and distance scales of membrane domain organization. *Mol. Membr. Biol*. 12:9–13.
8. Seelig, A., and J. Seelig. 1974. The dynamic structure of fatty acyl chains in a phospholipid bilayer measured by deuterium magnetic resonance. *Biochemistry*. 13:4839–4845.
9. Schindler, H., and J. Seelig. 1975. Deuterium order parameters in relation to thermodynamic properties of a phospholipid bilayer. A statistical mechanical interpretation. *Biochemistry*. 14:2283–2287.
10. Feller, S. E., D. Huster, and K. Gawrisch. 1999. Interpretation of NOESY cross-relaxation rates from molecular dynamics simulation of a lipid bilayer. *J. Am. Chem. Soc*. 121:8963–8964.
11. Brown, M. F., R. L. Thurmond, S. W. Dodd, D. Otten, and K. Beyer. 2002. Elastic deformation of membrane bilayers probed by deuterium NMR relaxation. *J. Am. Chem. Soc*. 124:8471–8484.
12. Rubenstein, J. L., B. A. Smith, and H. M. McConnell. 1979. Lateral diffusion in binary mixtures of cholesterol and phosphatidylcholines. *Proc. Natl. Acad. Sci. USA*. 76:15–18.
13. Lindblom, G., and G. Orädd. 1994. NMR studies of translational diffusion in lyotropic liquid crystals and lipid membranes. *Prog. NMR Spectrosc*. 26:483–515.
14. Gaede, H. C., and K. Gawrisch. 2003. Lateral diffusion rates of lipid, water, and a hydrophobic drug in a multilamellar liposome. *Biophys. J*. 85:1734–1740.
15. Davis, J. H. 1983. The description of membrane lipid conformation, order and dynamics by ^{2}H-NMR. *Biochim. Biophys. Acta*. 737: 117–171.
16. Tocanne, J. F., L. Dupoucezanne, A. Lopez, and J. F. Tournier. 1989. Lipid lateral diffusion and membrane organization. *FEBS Lett*. 257: 10–16.
17. Kapitza, H. G., D. A. Rüppel, H. J. Galla, and E. Sackmann. 1984. Lateral diffusion of lipids and glycophorin in solid phosphatidylcholine bilayers. The role of structural defects. *Biophys. J*. 45:577–587.
18. Stockton, G. W., and I. C. Smith. 1976. A deuterium nuclear magnetic resonance study of the condensing effect of cholesterol on egg phosphatidylcholine bilayer membranes. I. Perdeuterated fatty acid probes. *Chem. Phys. Lipids*. 17:251–263.
19. Davies, M. A., H. F. Schuster, J. W. Brauner, and R. Mendelsohn. 1990. Effects of cholesterol on conformational disorder in dipalmitoylphosphatidylcholine bilayers. A quantitative IR study of the depth dependence. *Biochemistry*. 29:4368–4373.
20. Reinl, H., T. Brumm, and T. M. Bayerl. 1992. Changes of the physical properties of the liquid-ordered phase with temperature in binary mixtures of DPPC with cholesterol. A ^{2}H-NMR, FT-IR, DSC, and neutron scattering study. *Biophys. J*. 61:1025–1035.
21. McIntosh, T. J., S. A. Simon, D. Needham, and C. H. Huang. 1992. Structure and cohesive properties of sphingomyelin/cholesterol bilayers. *Biochemistry*. 31:2012–2020.
22. Endress, E., H. Heller, H. Casalta, M. F. Brown, and T. M. Bayerl. 2002. Anisotropic motion and molecular dynamics of cholesterol, lanosterol, and ergosterol in lecithin bilayers studied by quasi-elastic neutron scattering. *Biochemistry*. 41:13078–13086.
23. Kusumi, A., W. K. Subczynski, M. Pasenkiewicz-Gierula, J. S. Hyde, and H. Merkle. 1986. Spin label studies on phosphatidylcholine-cholesterol membranes—effects of alkyl chain length and unsaturation in the fluid phase. *Biochim. Biophys. Acta*. 854:307–317.
24. Filippov, A., G. Orädd, and G. Lindblom. 2003. Influence of cholesterol and water content on phospholipid lateral diffusion in bilayers. *Langmuir*. 19:6397–6400.
25. Filippov, A., G. Orädd, and G. Lindblom. 2003. The effect of cholesterol on the lateral diffusion of phospholipids in oriented bilayers. *Biophys. J*. 84:3079–3086.
26. Scheidt, H. A., D. Huster, and K. Gawrisch. 2005. Diffusion of cholesterol and its precursors in lipid membranes studied by ^{1}H PFG MAS NMR. *Biophys. J*. 89:2504–2512.
27. Baumgart, T., S. T. Hess, and W. W. Webb. 2003. Imaging coexisting fluid domains in biomembrane models coupling curvature and line tension. *Nature*. 425:821–824.
28. Veatch, S. L., and S. L. Keller. 2003. Separation of liquid phases in giant vesicles of ternary mixtures of phospholipids and cholesterol. *Biophys. J*. 85:3074–3083.
29. Dietrich, C., B. Yang, T. Fujiwara, A. Kusumi, and K. Jacobson. 2002. Relationship of lipid rafts to transient confinement zones detected by single particle tracking. *Biophys. J*. 82:274–284.
30. Veatch, S. L., and S. L. Keller. 2002. Organization in lipid membranes containing cholesterol. *Phys. Rev. Lett*. 89:268101.
31. Dietrich, C., L. A. Bagatolli, Z. N. Volovyk, N. L. Thompson, M. Levi, K. Jacobson, and E. Gratton. 2001. Lipid rafts reconstituted in model membranes. *Biophys. J*. 80:1417–1428.
32. Bagatolli, L. A., and E. Gratton. 2000. A correlation between lipid domain shape and binary phospholipid mixture composition in free standing bilayers: a two-photon fluorescence microscopy study. *Biophys. J*. 79:434–447.
33. Korlach, J., P. Schwille, W. W. Webb, and G. W. Feigenson. 1999. Characterization of lipid bilayer phases by confocal microscopy and fluorescence correlation spectroscopy. *Proc. Natl. Acad. Sci. USA*. 96: 8461–8466.
34. Radhakrishnan, A., and H. McConnell. 2005. Condensed complexes in vesicles containing cholesterol and phospholipids. *Proc. Natl. Acad. Sci. USA*. 102:12662–12666.

35. Chachaty, C., D. Rainteau, C. Tessier, P. J. Quinn, and C. Wolf. 2005. Building up of the liquid-ordered phase formed by sphingomyelin and cholesterol. *Biophys. J.* 88:4032–4044.

36. Anderson, R. G. W., and K. Jacobson. 2002. Cell biology—a role for lipid shells in targeting proteins to caveolae, rafts, and other lipid domains. *Science.* 296:1821–1825.

37. Subczynski, W. K., and A. Kusumi. 2003. Dynamics of raft molecules in the cell and artificial membranes: approaches by pulse EPR spin labeling and single molecule optical microscopy. *Biochim. Biophys. Acta.* 1610:231–243.

38. Edidin, M. 2003. The state of lipid rafts: from model membranes to cells. *Annu. Rev. Biophys. Biomol. Struct.* 32:257–283.

39. Brown, D. A., and J. K. Rose. 1992. Sorting of GPI-anchored proteins to glycolipid-enriched membrane subdomains during transport to the apical cell-surface. *Cell.* 68:533–544.

40. Heerklotz, H. 2002. Triton promotes domain formation in lipid raft mixtures. *Biophys. J.* 83:2693–2701.

41. London, E., and D. A. Brown. 2000. Insolubility of lipids in Triton X-100: physical origin and relationship to sphingolipid/cholesterol membrane domains (rafts). *Biochim. Biophys. Acta.* 1508:182–195.

42. London, E. 2002. Insights into lipid raft structure and formation from experiments in model membranes. *Curr. Opin. Struct. Biol.* 12:480–486.

43. Veatch, S. L., I. V. Polozov, K. Gawrisch, and S. L. Keller. 2004. Liquid domains in vesicles investigated by NMR and fluorescence microscopy. *Biophys. J.* 86:2910–2922.

44. Sankaram, M. B., and T. E. Thompson. 1991. Cholesterol-induced fluid-phase immiscibility in membranes. *Proc. Natl. Acad. Sci. USA.* 88:8686–8690.

45. Bloom, M., E. E. Burnell, A. L. MacKay, C. P. Nichol, M. I. Valic, and G. Weeks. 1978. Fatty acyl chain order in lecithin model membranes determined from proton magnetic resonance. *Biochemistry.* 17:5750–5762.

46. Lichtenberg, D., N. O. Petersen, J. L. Girardet, M. Kainosho, P. A. Kroon, C. H. A. Seiter, G. W. Feigenson, and S. I. Chan. 1975. The interpretation of proton magnetic resonance linewidths for lecithin dispersions. Effect of particle size and chain packing. *Biochim. Biophys. Acta.* 382:10–21.

47. Oldfield, E., J. L. Bowers, and J. Forbes. 1987. High-resolution proton and ^{13}C NMR of membranes: why sonicate? *Biochemistry.* 26: 6919–6923.

48. Forbes, J., C. Husted, and E. Oldfield. 1988. High-field, high-resolution proton ''magic-angle'' sample-spinning nuclear magnetic resonance spectroscopic studies of gel and liquid crystalline lipid bilayers and the effects of cholesterol. *J. Am. Chem. Soc.* 110:1059–1065.

49. Polozov, I. V., and K. Gawrisch. 2004. Domains in binary SOPC/POPE lipid mixtures studied by pulsed field gradient ^{1}H MAS NMR. *Biophys. J.* 87:1741–1751.

50. Dai, M. C., H. B. Chiche, N. Düzgünes, E. Ayanoglu, and C. Djerassi. 1991. Phospholipid studies of marine organisms: 26. Interactions of some marine sterols with 1-stearoyl-2-oleoyl phosphatidylcholine (SOPC) in model membranes. *Chem. Phys. Lipids.* 59:245–253.

51. Vilcheze, C., T. P. W. McMullen, R. N. McElhaney, and R. Bittman. 1996. The effect of side-chain analogues of cholesterol on the thermotropic phase behavior of 1-stearoyl-2-oleoylphosphatidylcholine bilayers: a differential scanning calorimetric study. *Biochim. Biophys. Acta.* 1279:235–242.

52. Davis, P. J., and K. M. W. Keough. 1983. Differential scanning calorimetric studies of aqueous dispersions of mixtures of cholesterol with some mixed-acid and single-acid phosphatidylcholines. *Biochemistry.* 22:6334–6340.

53. Koynova, R., and M. Caffrey. 2002. An index of lipid phase diagrams. *Chem. Phys. Lipids.* 115:107–219.

54. Boden, N., and Y. K. Levine. 1978. Calculation of NMR spin-echo responses in solids. *J. Magn. Reson.* 30:327–342.

55. Volke, F., K. Arnold, and K. Gawrisch. 1982. The effect of hydration on the mobility of phospholipids in the gel state—a proton nuclear magnetic resonance spin echo study. *Chem. Phys. Lipids.* 31:179–189.

56. Nagle, J. F., Y. F. Liu, S. Tristram-Nagle, R. M. Epand, and R. E. Stark. 1999. Re-analysis of magic angle spinning nuclear magnetic resonance determination of interlamellar waters in lipid bilayer dispersions. *Biophys. J.* 77:2062–2065.

57. Zhou, Z., B. G. Sayer, D. W. Hughes, R. E. Stark, and R. M. Epand. 1999. Studies of phospholipid hydration by high-resolution magic-angle spinning nuclear magnetic resonance. *Biophys. J.* 76:387–399.

58. Boden, N., P. J. Jackson, Y. K. Levine, and A. J. I. Ward. 1976. Intramolecular disorder and its relation to mesophase structure in lyotropic liquid crystals. *Chem. Phys. Lett.* 37:100–105.

59. Linseisen, F. M., J. L. Thewalt, M. Bloom, and T. M. Bayerl. 1993. ^{2}H-NMR and DSC study of SEPC-cholesterol mixtures. *Chem. Phys. Lipids.* 65:141–149.

60. Thewalt, J. L., C. E. Hanert, F. M. Linseisen, A. J. Farrall, and M. Bloom. 1992. Lipid-sterol interactions and the physical properties of membranes. *Acta Pharm.* 42:9–23.

61. Davis, J. H. 1979. Deuterium magnetic resonance study of the gel and liquid crystalline phases of dipalmitoylphosphatidylcholine. *Biophys. J.* 27:339–358.

62. Bienvenue, A., M. Bloom, J. H. Davis, and P. F. Devaux. 1982. Evidence for protein-associated lipids from deuterium nuclear magnetic resonance studies of rhodopsin- dimyristoylphosphatidylcholine recombinants. *J. Biol. Chem.* 257:3032–3038.

63. Maricq, M. M., and J. S. Waugh. 1979. NMR in rotating solids. *J. Chem. Phys.* 70:3300–3316.

64. Forbes, J., J. Bowers, X. Shan, L. Moran, E. Oldfield, and M. A. Moscarello. 1988. Some new developments in solid-state nuclear magnetic resonance spectroscopic studies of lipids and biological membranes, including the effect of cholesterol in model and natural systems. *J. Chem. Soc., Faraday Trans. 1.* 84:3821–3849.